



# Thermodynamic-based comparison of ORC, TFC and OFC systems for waste heat recovery from a marine diesel engine

Mehtali Ketfi<sup>1</sup>, Mohamed Djermouni<sup>1</sup>, Ahmed Ouadha<sup>1,\*</sup>

## ARTICLE INFO

### Article history:

Received 13 Jul 2023;  
in revised from 24 Aug 2023;  
accepted 6 Oct 2023.

### Keywords:

Thermodynamic; Waste Heat Recovery; ORC; TFC; OFC; Marine Applications.

## ABSTRACT

The aim of this research is to comparatively evaluate the thermodynamic performance of three different systems, namely the organic Rankine cycle (ORC), trilateral flash cycle (TFC), and organic flash cycle (OFC), for the purpose of recovering waste heat on ships. To analyze their performance, simulations were conducted using specific working fluids with favorable thermophysical properties, namely n-butane (R600), i-butane (R600a), n-pentane (R601), i-pentane (R601a), and toluene. The results indicate that, within the operating parameters considered in this study, the ORC system achieves higher thermal efficiency compared to the TFC and OFC systems. However, the TFC system exhibits the advantage of a lower specific volume of the working fluid at the end of the heat addition process (expander inlet) since it remains in a liquid state. This characteristic allows for the use of smaller-sized expanders, making the TFC system particularly appealing for marine applications. Furthermore, it was observed that all the selected working fluids outperform R245fa in terms of power generation within the ORC system. In the case of the TFC and OFC systems, only R601, R601a, and toluene surpass the performance of R245fa.

© SECMAR | All rights reserved

## Nomenclature.

$\dot{Q}$ : Heat transfer rate (kW).  
 $s$ : Entropy (kJ/kgK).  
 $T$ : Temperature (K).  
 $v$ : Specific volume (m<sup>3</sup>/kg).  
 $x$ : Quality.  
 $h$ : Specific enthalpy (kJ/kg).  
 $\dot{m}$ : Mass flow rate (kg/s).  
 $p$ : Pressure (bar).  
 $\dot{W}$ : Power (kW).

### Greek symbols.

$\eta$ : Isentropic efficiency.

$\rho$ : Density (kg/m<sup>3</sup>).

### Subscripts.

*cond*: Condenser.  
*evap*: Evaporator/Heater.  
*exp*: Expander.  
*f*: Fluid.  
*p*: Pump.  
*th*: Thermal.

## 1. Introduction.

Traditional marine propulsion systems encounter challenges related to energy and environmental issues, specifically the imperative to decrease air pollution and carbon emissions. To tackle these concerns, waste heat recovery (WHR) systems are considered a viable solution. Notably, the organic Rankine cycle (ORC), a proven technology for converting low-grade heat into usable power, has garnered interest for recovering waste heat from marine diesel engines. Studies have demonstrated

<sup>1</sup>Laboratoire des Sciences et Ingénierie Maritimes, Faculté de Génie Mécanique, Université des Sciences et de la Technologie Mohamed Boudiaf d'Oran, B.P. 1505 Oran El-Mnouar, 31000 Oran, Algérie.

\*Corresponding author: A. Ouadha. E-mail Address: ah\_ouadha@yahoo.fr.

that implementing ORC systems on ships can lead to fuel savings of at least 3%, with a payback period of approximately 4 years (Konur et al., 2022).

The majority of prior research on waste heat recovery (WHR) power systems in marine settings primarily concentrated on the organic Rankine cycle (ORC) due to its established and mature status as a technology for extracting energy from low-grade heat sources (Bounefour, 2021). However, there have been investigations into other WHR power systems as well (Larsen et al., 2014; Zhang et al., 2022). For a more comprehensive understanding, interested readers can consult review papers that delve deeper into this subject (Shu et al., 2013; Singh and Pedersen, 2016; Mondejar et al., 2018; Konur et al., 2022).

In contrast, the trilateral flash cycle (TFC) and the organic flash cycle (OFC) have received relatively less attention in the context of marine applications. Choi and Kim (2013) proposed a waste heat recovery system that integrates a trilateral cycle and an organic Rankine cycle on a 6800 TEU container ship. The results demonstrated a propulsion efficiency improvement of 2.824% compared to a baseline engine. Rijpkema et al. (2019) conducted simulations for fifty different working fluids and four WHR cycles, both with and without a recuperator, including an ORC, a TRC, a TFC, and an OFC. These systems were simulated using various heat sources from a heavy-duty diesel engine. The results highlighted significant performance variations among the simulated scenarios. The maximum power output was achieved by harnessing heat from the charge air cooler, exhaust, and EGR cooler using ORC and TRC systems with working fluids such as acetone, methanol, cyclopentane, ethanol, or isohexane.

The aforementioned literature underscores the predominant focus on ORC-based power cycles for waste heat recovery from marine engines, while relatively few studies have specifically compared ORC-based configurations like TFC and OFC. Therefore, this paper conducts a thermodynamic comparison of ORC, TFC, and OFC systems to identify the optimal choice for waste heat recovery from marine engines.

## 2. Methodology.

### 2.1. The marine engine.

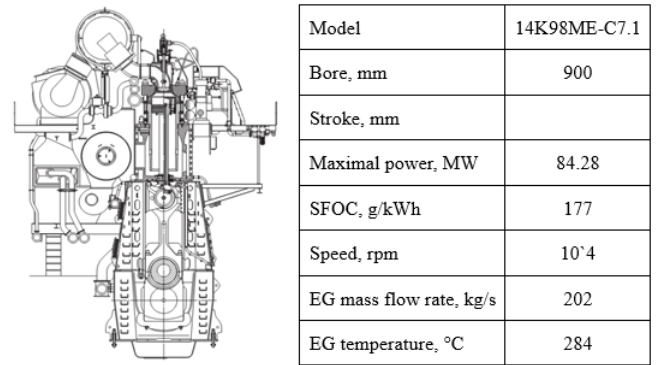
Figure 1 illustrates a cross-sectional view of the engine analyzed in this study, along with its corresponding specifications. The engine in question is a two-stroke marine diesel engine with 14 cylinders, capable of generating a maximum power output of 84.28 MW at a rotational speed of 104 rpm (Man, 2014).

### 2.2. Description of the systems.

Figure 2 displays the schematics and corresponding cycles, depicted on T-s (temperature-entropy) diagrams, for the three waste heat recovery (WHR) power systems examined in this study: ORC, TFC, and OFC.

All three systems share a common initial phase in the cycle, which involves the compression of the liquid by the pump (1-2) and the process of isobaric heat addition (2-3). The point

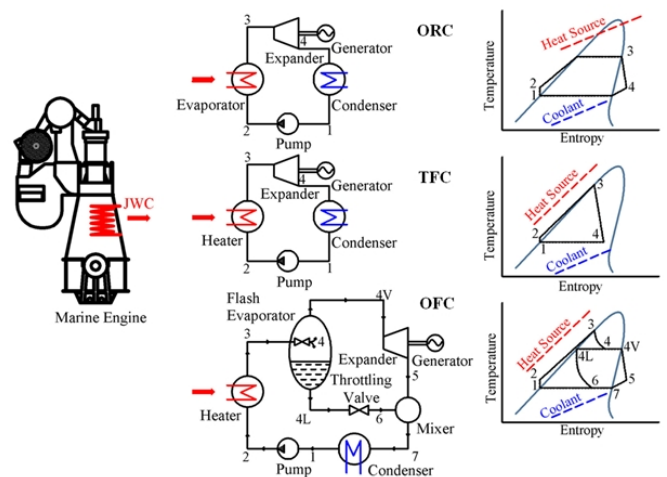
Figure 1: Cross section and specifications of the engine used.



Source: Authors.

of differentiation between the systems arises when the working fluid reaches the high-pressure saturated liquid state (3). In an ORC system, the expansion of the working fluid commences from the high-pressure saturated vapor state (3-4). In contrast, in a TFC system, the expansion begins directly from the high-pressure saturated state, leading to a low-pressure two-phase state (3-4). As for the OFC system, prior to expansion, the working fluid undergoes a flashing process, transitioning to an intermediate pressure and separating into saturated liquid (4L) and saturated vapor (4V). The saturated vapor then expands to generate useful work (4V-5). Simultaneously, the saturated liquid undergoes a throttling process (4L-6) and subsequently mixes with the expanded fluid (7). Finally, the working fluid is condensed back to a saturated state (7-1) to initiate a new cycle.

Figure 2: Schematics and corresponding T-s diagrams of the three power cycles studied.



Source: Authors.

Due to their favorable thermophysical characteristics, specifically high critical pressure and temperature, low specific volume, and latent heat, n-butane (R600), i-butane (R600a), n-pentane (R601), i-pentane (R601a), and toluene have been cho-

sen as the working fluids for the system under investigation. These fluids, as indicated in Table 1, are expected to deliver optimal performance due to their excellent properties. It is important to note that all of the selected working fluids are considered dry fluids.

Table 1: Properties and classification of the working fluids studied.

Working fluid	Type	$M$ (g/mol)	$T_b$ (K)	$T_c$ (K)	$p_c$ (MPa)	$GWP$
R245fa (C <sub>3</sub> H <sub>3</sub> F <sub>3</sub> )	Dry	152.9	300.99	427.20	3.65	950
n-Butane (C <sub>4</sub> H <sub>10</sub> )	Dry	58.12	272.65	425.15	3.80	4.0
i-Butane (C <sub>4</sub> H <sub>10</sub> )	Dry	58.12	261.45	407.85	3.63	3.0
n-Pentane (C <sub>5</sub> H <sub>12</sub> )	Dry	72.15	309.07	469.70	3.36	<3.0
i-Pentane (C <sub>5</sub> H <sub>12</sub> )	Dry	72.15	301.06	460.40	3.37	<3.0
Toluene (C <sub>7</sub> H <sub>8</sub> )	Dry	92.14	383.75	591.75	4.13	~3.3

Source: Authors.

### 2.3. Thermodynamic modeling.

The thermodynamic models employed in this study were established based on the following assumptions:

- All systems analyzed operate under steady-state conditions.
- Variations in kinetic and potential energy of the working fluid are disregarded.
- Pressure and heat losses are not taken into consideration.
- The performance of turbines and pumps is determined using isentropic efficiencies.

To develop the models, each component of the system is treated as a control volume, and mass, and energy balance equations are applied. With the aforementioned assumptions in mind, the mass and energy balance equations are formulated as follows:

$$\sum \dot{m}_{in} = \sum \dot{m}_{out} \quad (1)$$

$$\sum \dot{m}_{in} h_{in} + \sum \dot{Q} = \sum \dot{m}_{out} h_{out} + \sum \dot{W} \quad (2)$$

where,  $\dot{m}$  denote for the mass flow rate,  $h$  the enthalpy,  $\dot{Q}$  the heat transfer and  $\dot{W}$  is the mechanical power transfer. The subscripts *in* and *out* refer to the inlet and outlet of the control volume respectively.

Final expressions for mass and energy balance equations for each component of the systems are listed in Table 2.

Table 2: Energy balance equations.

Component	Energy balance equation	
ORC	Pump	$\dot{W}_p = \dot{m}_f (h_2 - h_1)$
	Evaporator	$\dot{Q}_{evap} = \dot{m}_f (h_3 - h_2)$
	Expander	$\dot{W}_{exp} = \dot{m}_f (h_3 - h_4)$
	Condenser	$\dot{Q}_{cond} = \dot{m}_f (h_4 - h_1)$
	System	$\dot{W}_{net} = \dot{W}_{exp} - \dot{W}_p$ $\eta_{th} = \dot{W}_{net} / \dot{Q}_b$
TFC	Pump	$\dot{W}_p = \dot{m}_f (h_2 - h_1)$
	Heater	$\dot{Q}_{evap} = \dot{m}_f (h_3 - h_2)$
	Expander	$\dot{W}_{exp} = \dot{m}_f (h_3 - h_{4s}) \eta_{nozzle} \eta_{rotor}$
		$\eta_{nozzle} = 0.865 + 0.00175 \cdot \rho_{4v}$ $\eta_{rotor} = 0.575 + 0.325 \cdot x_4$
	Condenser	$\dot{Q}_{cond} = \dot{m}_f (h_4 - h_1)$
System	$\dot{W}_{net} = \dot{W}_{exp} - \dot{W}_p$ $\eta_{th} = \dot{W}_{net} / \dot{Q}_b$	
OFC	Pump	$\dot{W}_p = \dot{m}_f (h_2 - h_1)$
	Heater	$\dot{Q}_{evap} = \dot{m}_f (h_3 - h_2)$
	Expander	$\dot{W}_{exp} = \dot{m}_f (h_3 - h_{4s})$
	Condenser	$\dot{Q}_{cond} = \dot{m}_f (h_4 - h_1)$
	System	$\dot{W}_{net} = \dot{W}_{exp} - \dot{W}_p$ $\eta_{th} = \dot{W}_{net} / \dot{Q}_b$

Source: Author.

where  $\rho_{4v}$  is the vapor density at the condensation pressure and  $x_4$  is the vapor quality at the nozzle exit.

The nozzle and rotor efficiencies have been developed taking into account the main influencing parameters for different working fluids (Welch and Boyle, 2009; Hays, 2010).

### 3. Results and Discussions.

This section focuses on comparing the performance of three power cycles: the basic organic Rankine cycle (ORC), the trilateral flash power cycle (TFC), and the organic flash power cycle (OFC). Simulations were conducted under predetermined operating conditions, which are presented in Table 3. To facilitate the analysis, a program was developed using Engineering Equation Solver (EES) (Klein and Nellis, 2012), taking into account the established model and assumptions described above.

The performances of the three systems are graphically presented in Figure 3, considering different working fluids. The comparisons are made based on three key factors: mechanical

Table 3: Operating conditions.

Heat source working fluid	PG
Heat source mass flow rate, kg/s	50
Heat source temperature, °C	80
ORC, TFC, OFC working fluid	R245fa, R600, R600a, R601, R601a, Toluene
Evaporator (Heater) temperature, °C	75
Condenser temperature, °C	30
Flash temperature, °C	(75+30)/2
Turbine isentropic efficiency, %	80
Pump isentropic efficiency, %	70

Source: Authors.

power generated, mass flow rate of the working fluid, and thermal efficiency.

The ORC system demonstrates the highest heat input to the system due to the heating, vaporization, and superheating of the working fluid. However, within the specified operating parameters, the ORC system achieves the highest power output ranging from 80.55 kW to 89.30 kW.

Following that, the TFC system yields a power output ranging from 30.21 kW to 35.01 kW, and the OFC system produces power ranging from 27.09 kW to 27.95 kW, as depicted in Figure 3(a).

Consequently, in terms of thermal efficiency, the ORC system outperforms both the TFC and OFC systems, as illustrated in Figure 3(c).

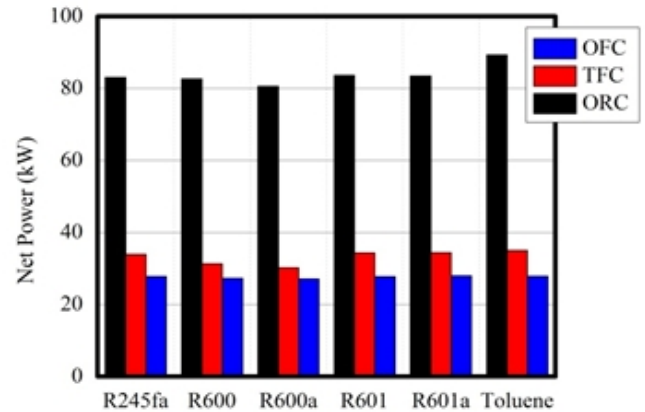
Notably, in the case of the ORC system, all of the selected working fluids result in higher power output compared to R245fa. However, for the TFC and OFC systems, only R601, R601a, and toluene surpass the performance of R245fa.

Within the considered operating conditions of this study, the ORC system exhibits lower mass flow rates of the working fluid compared to the TFC and OFC systems. Conversely, the TFC and OFC systems demonstrate similar mass flow rates across all the considered working fluids.

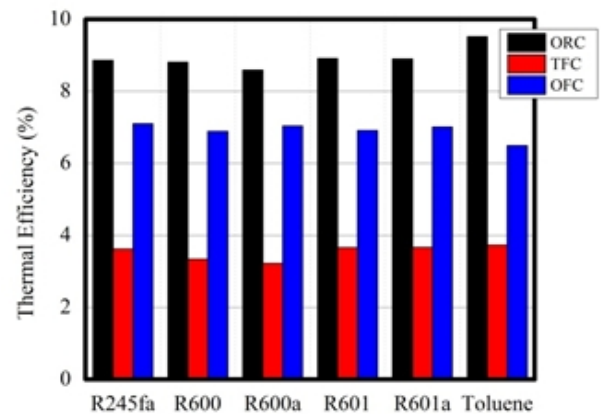
The TFC system, with its working fluid remaining in a liquid state, results in a lower specific volume at the end of the heat addition process (expander inlet). On the other hand, the OFC system, with its working fluid undergoing flashing to an intermediate pressure and separation into saturated liquid and vapor, exhibits a significantly higher volume of working fluid flowing through the expander.

Consequently, the TFC systems require smaller-sized expanders compared to the OFC systems. This reduced system size holds significant importance for marine applications. Aside from the space-saving benefits onboard ships, a smaller-sized system substantially decreases material costs.

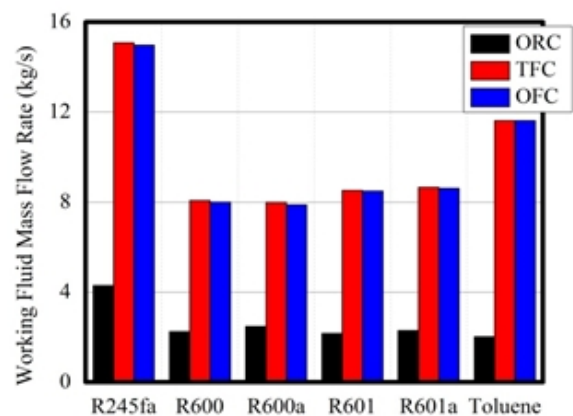
Figure 3: Performance comparison among systems: (a) Power output; (b) Mass flow rate; (c) Thermal efficiency.



(a)



(b)



Source: Authors.

### Conclusions.

A comparative analysis of three waste heat recovery technologies, namely ORC, TFC, and OFC, was conducted in terms

of power output, thermal efficiency, and volumetric mass flow rate supplied to the expander. Simulations were carried out using different working fluids, including R245fa, butane, isobutane, pentane, isopentane, and toluene. The main conclusions drawn from this study are summarized as follows:

- The ORC system demonstrates superior performance compared to both the TFC and OFC systems.
- With the exception of butane and isobutane, which exhibit slightly lower performance than R245fa, the other working fluids (pentane, isopentane, and toluene) consistently deliver better performance across all systems.
- Due to the TFC system's working fluid remaining in a liquid state, there is a reduced specific volume at the end of the heat addition process (expander inlet). As a result, TFC systems require smaller-sized expanders in comparison to OFC systems. This characteristic makes TFC systems particularly advantageous for marine applications.

## References.

- Bounefour, O., 2021, Valorisation des rejets de chaleur des moteurs diesel marins, PhD Thesis, USTO-MB, Algeria. [http://www.univ-usto.dz/theses\\_en\\_ligne/index.php?lvl=notice\\_display&id=5374](http://www.univ-usto.dz/theses_en_ligne/index.php?lvl=notice_display&id=5374).
- Choi, B.C., and Kim, Y.M., 2013, Thermodynamic analysis of a dual loop heat recovery system with trilateral cycle applied to exhaust gases of internal combustion engine for propulsion of the 6800 TEU container ship, *Energy*, **58**, pp. 404–416. <https://doi.org/10.1016/j.energy.2013.05.017>.
- Hays, L., 2010, Demonstration of a variable phase turbine power system for low temperature geothermal sources. U.S. Department of energy. Geothermal Technologies Program, Report Number G015153.
- Klein, S., and Nellis, G., 2012, Mastering EES, f-Chart software. <https://fchartsoftware.com/ees/mastering-ees.php>.
- Konur, O., Colpan, C.O., and Saatcioglu, O.Y., 2022, A comprehensive review on organic Rankine cycle systems used as waste heat recovery technologies for marine applications, *Energy Sources, Part A: Recovery, Utilization, and Environmental Effects*, **44**, pp. 4083–4122. <https://doi.org/10.1080/15567036.2022.2072981>.
- Larsen, U., Nguyen, T.-V., Knudsen, T., and Haglind, F., 2014, System analysis and optimisation of a Kalina split-cycle for waste heat recovery on large marine diesel engines, *Energy*, **64**, pp. 484–494. <https://doi.org/10.1016/j.energy.2013.10.069>.
- Man, 2014, MAN B&W K98ME-C7.1-TII, Project guide electronically controlled two stroke engines. <https://man-es.com/applications/projectguides/2stroke/content/printed/k98mec7.pdf>.
- Mondejar, M.E., Andreasen, J.G., Pierobon, L., Larsen, U., et al., 2018, A review of the use of organic Rankine cycle power systems for maritime applications, *Renew. Sustain. Energy Rev.*, **91**, pp. 126–151. <https://doi.org/10.1016/j.rser.2018.03.074>.
- Rijpkema, J., Munch, K., and Andersson, S.B., 2019, Combining Low - and High-Temperature Heat Sources in a Heavy Duty Diesel Engine for Maximum Waste Heat Recovery Using Rankine and Flash Cycles, In: Junior, C., Dingel, O. (eds) *Energy and Thermal Management, Air-Conditioning, and Waste Heat Utilization*. ETA 2018. Springer, Cham. [https://doi.org/10.1007/978-3-030-00819-2\\_12](https://doi.org/10.1007/978-3-030-00819-2_12).
- Shu, G., Liang, Y., Wei, H., Tian, H., Zhao, J., Liu, L., 2013, A review of waste heat recovery on two-stroke IC engine aboard ships, *Renew. Sustain. Energy Rev.*, **19**, pp. 385–401. <https://doi.org/10.1016/j.rser.2012.11.034>.
- Singh, D.V., and Pedersen, E., 2016, A review of waste heat recovery technologies for maritime applications, *Energy Convers. Manag.*, **111**, pp. 315–328. <https://doi.org/10.1016/j.enconman.2015.12.073>.
- Welch, P., and Boyle, P., 2009, New turbines to enable efficient geothermal power plants, *Geothermal Resources Council Transactions*, **33**, pp. 765–772. [http://www.energent.net/documents/Geothermal\\_Resources\\_Council\\_2009\\_Paper.pdf](http://www.energent.net/documents/Geothermal_Resources_Council_2009_Paper.pdf).
- Zhang, X., Cao, M., He, M. and Wang, J., 2022, Thermodynamic and Economic Studies of a Combined Cycle for Waste Heat Recovery of Marine Diesel Engine, *Journal of Thermal Science*, **31**, pp. 417–435. <https://doi.org/10.1007/s11630-020-1351-x>.